Dalton Transactions

COMMUNICATION

View Article Online
View Journal | View Issue

Cite this: *Dalton Trans.*, 2020, **49**, 3658

Received 8th May 2019,
Accepted 25th June 2019

DOI: 10.1039/c9dt01911a

rsc.li/dalton

A microporous metal–organic framework with naphthalene diimide groups for high methane storage†

Yingxiang Ye, [a,b] Rui-Biao Lin, [b] Hui Cui,[b] Ali Alsalme,[c] Wei Zhou, [d] Taner Yildirim,[d] Zhangjing Zhang,*[a] Shengchang Xiang [a] and Banglin Chen *[b]

We reported a microporous MOF FJU-101 with open naphthalene diimide functional groups for room temperature (RT) high methane storage. At RT and 65 bar, the total volumetric CH_4 storage capacity of 212 cm^3 (STP) cm^{-3} of FJU-101a is significantly higher than those of the isoreticular MFM-130a and UTSA-40a. The enhanced methane uptake in FJU-101a is attributed to the polar carbonyl sites, which can generate strong electrostatic interactions with CH_4 molecules.

Due to the rapid development of global economy, the demand for fossil fuel is growing rapidly. Natural gas (NG), consisting of approximately 95% methane (CH_4), is considered as a promising alternative energy source that is clean and renewable,[1,2] because of its abundant reserves and lower CO_2 emissions than conventional petroleum-based fuels. To fully promote the use of natural gas as fuel for vehicles, there is an urgent demand to seek suitable adsorbents that can display a high CH_4 storage and working capacity at relatively low pressure.[3,4] Recently, the US Department of Energy (DOE) has set an ambitious target for methane storage, with the gravimetric and volumetric storage capacities up to 0.5 g (CH_4) g^{-1} (adsorbent) and 350 cm^3 (STP) cm^{-3}, respectively, at room temperature.[5]

Compared with the conventional solid adsorbents (zeolites[6] and activated carbons[7]), the emergence of new types of crystalline materials, metal–organic frameworks (MOFs),[8] appears to be particularly promising for such applications,[9–14] attributed to their high porosities,[15] functional pore surfaces,[16–22] and versatile chemical features.[23–29] Notably, the volumetric CH_4 storage capacity may be more important than the gravimetric one, since the vehicles have limited space for gas tanks. To achieve high volumetric methane storage, it is not only necessary to balance the trade-off between porosity and framework density in MOFs, but also to incorporate functional sites to tune the interaction between methane molecules and the host MOF lattice. It has been well demonstrated that several promising strategies can significantly improve the volumetric CH_4 storage capacity, such as optimizing pore spaces,[30,31] incorporating open metal or Lewis basic functional sites,[32–35] and tuning the flexibility of the host framework.[36–39] The well-known MOF HKUST-1 exhibits the highest volumetric methane storage capacity of 267 cm^3 (STP) cm^{-3} at RT and 65 bar,[30] attributed to its suitable pore cavity and high density of open Cu sites. After this, our group reported a unique MOF (named UTSA-76, the NOTT-101 isomer) containing the dynamic pyrimidine group. It shows a record high methane working capacity of 197 cm^3 (STP) cm^{-3},[33] which is significantly higher than NOTT-101 of 181 cm^3 (STP) cm^{-3} at RT and 65 bar. Recently, Long and co-workers realized a usable CH_4 capacity of 197 cm^3 (STP) cm^{-3} at RT and 65 bar by employing a flexible MOF Co(bdp),[36] which might provide a new route to overcome volumetric storage limitations in rigid MOFs.

In the present study, we employed naphthalene diimide (NDI)-based tetracarboxylic acid (H_4L = *N*,*N*′-bis(5-isophthalic acid)naphthalenediimide) and $Cu(NO_3)_2$ to construct a three-dimensional porous MOF (**FJU-101**) under solvothermal conditions, based on the following considerations: (i) copper paddle-wheel $Cu_2(COO)_4$ clusters were easily assembled from *m*-benzenedicarboxylate and Cu^{2+}, while affording open Cu sites;[40] (ii) the tetratopic linkers connect with the paddle-wheel units to easily form the nanosize pore cavity, which facilitates gas storage, especially for methane;[32] (iii) the immobilized carbonyl groups can serve as secondary functional sites to increase the gas storage capacity in the high-pressure area. As expected, the activated **FJU-101a** exhibits a high methane storage capacity of 212 (or 181) cm^3 (STP) cm^{-3}

[a]*Fujian Provincial Key Laboratory of Polymer Materials, College of Chemistry and Materials Science, Fujian Normal University, 32 Shangsan Road, Fuzhou 350007, PR China. E-mail: zzhang@fjnu.edu.cn*
[b]*Department of Chemistry, University of Texas at San Antonio, One UTSA Circle, San Antonio, Texas 78249-0698, USA. E-mail: banglin.chen@utsa.edu*
[c]*Chemistry Department, College of Science, King Saud University, P O Box 2455, Riyadh 11451, Saudi Arabia*
[d]*Center for Neutron Research, National Institute of Standards and Technology, Gaithersburg, Maryland 20899-6102, USA*

†Electronic supplementary information (ESI) available: Additional gas adsorption isotherms and PXRD patterns. See DOI: 10.1039/c9dt01911a

at RT and 65 (or 35) bar, which is higher than those of MFM-130a of 176 (or 163) cm^3 (STP) cm^{-3}, and UTSA-40a of 192 (or 156) cm^3 (STP) cm^{-3}, in the same type of MOF.[41,42] In addition, at 77 K, the hydrogen (H_2) storage capacity in **FJU-101a** can reach 2.46 wt% (20.86 g L^{-1}) and 6.1 wt% (51.74 g L^{-1}) at 1 and 100 bar, respectively.

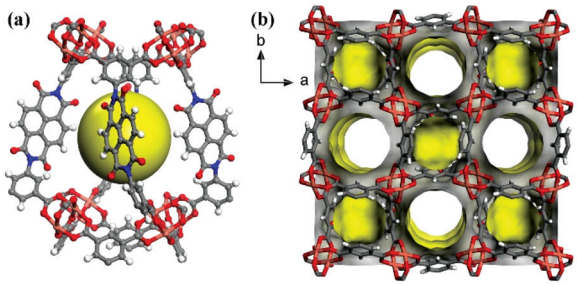

Fig. 1 Single crystal structure of **FJU-101**: (a) a spherical-like $[Cu_{16}(L)_4]$ nano-sized cage; (b) the 3D framework structure with a 1D cylindrical channel viewed along the crystallographic *c*-axis.

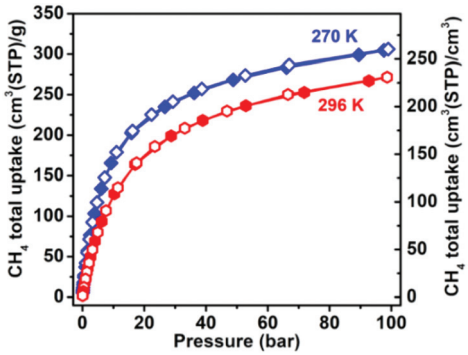

Fig. 2 High-pressure methane adsorption isotherms of **FJU-101a** at 270 K and 296 K. Solid symbols: adsorption; open symbols: desorption.

Green block-shaped crystals of **FJU-101** were synthesized with high yield by using a previously reported procedure.[43] As shown in Fig. 1, the single crystal structure shows that **FJU-101** has an approximately spherical-like nano-sized cage with a diameter of 9 Å, and possesses one-dimensional (1D) cylindrical channels with the dimensions of 7.5 × 7.5 $Å^2$ along the *c*-axis (taking into account the van der Waals radii of the atoms). The total accessible volume in **FJU-101** was calculated to be 65% using PLATON software, when the solvent molecules were not considered. Moreover, the phase purity of the bulk sample was proved using the powder X-ray diffraction (PXRD) patterns (Fig. S1†).

It is worth noting that **FJU-101a** displays a moderately high Brunauer–Emmett–Teller (BET) surface area and pore volume of 1909 m^2 g^{-1} and 0.762 cm^3 g^{-1}, respectively, and incorporates potential functional sites (open metal and carbonyl group sites) and suitable pore cavities, thus it might be a promising porous material for methane storage. To further investigate its potential applications in methane storage, high-pressure CH_4 adsorption isotherms were obtained from 0 to 100 bar at 270 and 296 K, respectively, as shown in Fig. 2. At 296 K and 35 bar, the total volumetric methane (CH_4) uptake of **FJU-101a** is 181 cm^3 (STP) cm^{-3}, which has surpassed the DOE's previous target of 180 cm^3 (STP) cm^{-3}, while ignoring the loss of packing density. After that, when the storage pressure further increases to 65 and 100 bar, the total volumetric methane uptake value can reach up to 212 and 259 cm^3 (STP) cm^{-3}, respectively. At room temperature, the total CH_4 uptake value at 35 and 65 bar is lower than those of some widely studied porous MOFs, such as HKUST-1 (227 and 267 cm^3 (STP) cm^{-3})[30] and UTSA-76a (211 and 257 cm^3 (STP) cm^{-3}),[33] but it is still higher than those of MFM-130a (163 and 176 cm^3 (STP) cm^{-3}),[41] UTSA-40a (156 and 192 cm^3 (STP) cm^{-3}),[42] and

Table 1 Comparison of some reported MOFs for high-pressure methane storage at room temperature

			Methane adsorption at 65 (35) bar		
MOFs	D_c [a]/g cm^{-3}	V_p [b]/cm^3 g^{-1}	Uptake[c]/cm^3 cm^{-3}	Delivery[d]/cm^3 cm^{-3}	CH_4 density[e] at 65 (35) bar/g cm^{-3}
NOTT-100a[32]	0.927	0.677	230 (195)	139 (104)	0.262 (0.222)
NOTT-109a[32]	0.79	0.85	242 (196)	170 (125)	0.257 (0.208)
UTSA-40a[42]	0.827	0.65	192 (156)	138 (102)	0.255 (0.207)
UTSA-76a[33]	0.699	1.09	257 (211)	197 (151)	0.241 (0.198)
FJU-101a	0.846	0.762	212 (181)	144 (113)	0.235 (0.200)
PCN-14[30]	0.829	0.85	230 (195)	157 (122)	0.233 (0.198)
NJU-Bai 43[45]	0.639	1.22	254 (202)	198 (146)	0.233 (0.185)
NOTT-101a[32]	0.684	1.08	239 (194)	183 (138)	0.231 (0.188)
NOTT-102a[32]	0.587	1.268	237 (181)	192 (136)	0.227 (0.174)
NOTT-103a[32]	0.643	1.157	236 (193)	183 (140)	0.226 (0.185)
ZJU-5a[46]	0.679	1.074	228 (190)	168 (130)	0.223 (0.186)
ZJU-25a[47]	0.622	1.183	229 (180)	181 (132)	0.222 (0.175)
MFM-130a[41]	0.642	1.0	176 (163)	131 (118)	0.196 (0.181)
ZJU-32a[48]	0.434	1.482	140 (97)	120 (77)	0.155 (0.108)

[a] D_c: crystal density (g cm^{-3}). [b] V_p: pore volume (cm^3 g^{-1}). [c] Total volumetric CH_4 uptake (cm^3 cm^{-3}). [d] The deliverable amount is defined as the difference in the total uptake between 65 (or 35) and 5 bar (cm^3 cm^{-3}). [e] CH_4 packing density in MOFs (g cm^{-3}), defined as $\rho_{CH_4} = Q_{CH_4}/V_p$, where Q_{CH_4} is the CH_4 uptake value (g g^{-1}) at 65 or 35 bar and V_p is the pore volume (cm^3 g^{-1}).

SNU-50a (153 cm^3 (STP) cm^{-3}, at 35 bar)[44] in the same type of MOF. Notably, the CH_4 storage capacity of **FJU-101a** is lower than that of some isoreticular MOFs with a larger pore volume, but the CH_4 packing density ($\rho_{CH_4} = Q_{CH_4}/V_p$) in our sample is higher than those of most widely studied MOFs (Table 1). It indicates that the accessible carbonyl groups can serve as secondary functional sites to increase the CH_4 storage capacity, as further proved by GCMC simulations (see the ESI† for details).

The CH_4 working capacity (also known as the deliverable capacity) is another important factor when considering an adsorbent for practical CH_4 storage. Generally, it is defined as the difference in total uptake between 65 (or 35) and 5 bar, which is more reasonable than the total storage capacity. The CH_4 working capacity of **FJU-101a** at 296 K is 144 (or 113) cm^3 (STP) cm^{-3}, which is also higher than those of MFM-130a and UTSA-40a of 131 (or 118) cm^3 (STP) cm^{-3} and 138 (or 102) cm^3 (STP) cm^{-3}, respectively.[41,42] In order to systematically compare the methane storage performance among the same types of MOFs as **FJU-101a**, all of the high-pressure CH_4 adsorption data from this work and other related references are summarized in Table 1.

To gain better insight into the superior methane storage performances, we calculated the adsorption enthalpy (Q_{st}) of **FJU-101a** from the isotherms collected at 270 and 296 K. Fig. S6† presents that the Q_{st} value of CH_4 adsorption at zero coverage is 17.3 kJ mol^{-1}, which is comparable to those of MFM-130a (16.0 kJ mol^{-1}),[41] NOTT-102 (16.0 kJ mol^{-1}),[32] and PCN-14 (18.7 kJ mol^{-1}).[30]

Considering that open Cu(II) sites can serve as strong H_2 binding sites, we also performed high pressure H_2 adsorption (0–100 bar) at various temperatures. At 77 K, **FJU-101a** can adsorb hydrogen of 2.46 wt% (20.86 g L^{-1}) and 6.1 wt% (51.74 g L^{-1}) at 1 and 100 bar (Fig. 3), respectively, higher than most well-known MOFs without open metal sites under the same conditions.[49,50] In addition, the total H_2 adsorption at RT and 100 bar is 1.1 wt%. The isosteric heat of adsorption of H_2 in **FJU-101a** was calculated to be 6.13 kJ mol^{-1} at zero coverage by employing the virial method (Fig. S8†).

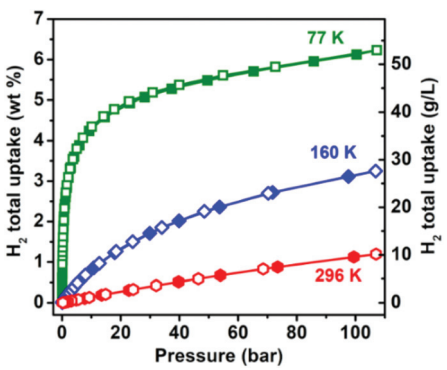

Fig. 3 High-pressure hydrogen adsorption isotherms of **FJU-101a** at 77 K, 160 K, and 296 K. Solid and open symbols represent adsorption and desorption, respectively.

Conclusions

In summary, we realized a microporous MOF (**FJU-101a**) with naphthalene diimide functional groups for room temperature high methane storage. Notably, at RT and 65 bar, **FJU-101a** displays a much higher volumetric CH_4 storage capacity of 212 cm^3 (STP) cm^{-3} in comparison with the isoreticular MFM-130a and UTSA-40a. The enhanced CH_4 storage capacity of **FJU-101a** is attributed to the polar carbonyl sites which can generate strong electrostatic interactions with CH_4 molecules. Our discovery would provide a new route to improve the gas storage capacity in MOFs by incorporating some specific functional sites to tune the interactions between the target gas molecules and the host framework.

Conflicts of interest

The authors declare no competing financial interest.

Acknowledgements

This work was financially supported by the National Natural Science Foundation of China (21673039, 21573042, and 21273033), the Fujian Science and Technology Department (2018J07001, 2016J01046, and 2014J06003), the Welch Foundation (AX-1730), and the Distinguished Scientist Fellowship Program (DSFP) at KSU. Y. Y. gratefully acknowledges the support of the China Scholarship Council.

Notes and references

1 R. F. Service, *Science*, 2014, **346**, 538.
2 R. A. Alvarez, S. W. Pacala, J. J. Winebrake, W. L. Chameides and S. P. Hamburg, *Proc. Natl. Acad. Sci. U. S. A.*, 2012, **109**, 6435–6440.
3 J. Wegrzyn and M. Gurevich, *Appl. Energy*, 1996, **55**, 71–83.
4 K. V. Kumar, K. Preuss, M.-M. Titirici and F. Rodríguez-Reinoso, *Chem. Rev.*, 2017, **117**, 1796–1825.
5 See DOE MOVE program at https://arpa-e-foa.energy.gov/.
6 S. Y. Zhang, O. Talu and D. T. Hayhurst, *J. Phys. Chem.*, 1991, **95**, 1722–1726.
7 M. E. Casco, M. Martínez-Escandell, E. Gadea-Ramos, K. Kaneko, J. Silvestre-Albero and F. Rodríguez-Reinoso, *Chem. Mater.*, 2015, **27**, 959–964.
8 H. Furukawa, K. E. Cordova, M. O'Keeffe and O. M. Yaghi, *Science*, 2013, **341**, 1230444.
9 J. A. Mason, M. Veenstra and J. R. Long, *Chem. Sci.*, 2014, **5**, 32–51.
10 Y. He, W. Zhou, G. Qian and B. Chen, *Chem. Soc. Rev.*, 2014, **43**, 5657–5678.
11 B. Li, H.-M. Wen, W. Zhou, J. Q. Xu and B. Chen, *Chem*, 2016, **1**, 557–580.
12 Y. He, F. Chen, B. Li, G. Qian, W. Zhou and B. Chen, *Coord. Chem. Rev.*, 2018, **373**, 167–198.

13 R.-B. Lin, S. Xiang, B. Li, Y. Cui, G. Qian, W. Zhou and B. Chen, *Coord. Chem. Rev.*, 2019, **384**, 21–36.
14 C. Song, H. Liu, J. Jiao, D. Bai, W. Zhou, T. Yildirim and Y. He, *Dalton Trans.*, 2016, **45**, 7559–7562.
15 O. K. Farha, I. Eryazici, N. C. Jeong, B. G. Hauser, C. E. Wilmer, A. A. Sarjeant, R. Q. Snurr, S. T. Nguyen, A. Ö. Yazaydın and J. T. Hupp, *J. Am. Chem. Soc.*, 2012, **134**, 15016–15021.
16 Y. Ye, Z. Ma, R.-B. Lin, R. Krishna, W. Zhou, Q. Lin, Z. Zhang, S. Xiang and B. Chen, *J. Am. Chem. Soc.*, 2019, **141**, 4130–4136.
17 T.-L. Hu, H. Wang, B. Li, R. Krishna, H. Wu, W. Zhou, Y. Zhao, Y. Han, X. Wang, W. Zhu, Z. Yao, S. Xiang and B. Chen, *Nat. Commun.*, 2015, **6**, 7328.
18 Y.-H. Han, Y. Ye, C. Tian, Z. Zhang, S.-W. Du and S. Xiang, *J. Mater. Chem. A*, 2016, **4**, 18742–18746.
19 S.-J. Bao, R. Krishna, Y.-B. He, J.-S. Qin, Z.-M. Su, S.-L. Li, W. Xie, D.-Y. Du, W.-W. He, S.-R. Zhang and Y.-Q. Lan, *J. Mater. Chem. A*, 2015, **3**, 7361–7367.
20 Y. Ye, H. Zhang, L. Chen, S. Chen, Q. Lin, F. Wei, Z. Zhang and S. Xiang, *Inorg. Chem.*, 2019, **58**, 7754–7759.
21 H. Cui, S. Chen, H. Arman, Y. Ye, A. Alsalme, R.-B. Lin and B. Chen, *Inorg. Chim. Acta*, 2019, **495**, 118938.
22 J. Zhang, J. Ouyang, Y. Ye, Z. Li, Q. Lin, T. Chen, Z. Zhang and S. Xiang, *ACS Appl. Mater. Interfaces*, 2018, **10**, 27465–27471.
23 R. B. Lin, L. Li, H. L. Zhou, H. Wu, C. He, S. Li, R. Krishna, J. Li, W. Zhou and B. Chen, *Nat. Mater.*, 2018, **17**, 1128–1133.
24 L. Li, R.-B. Lin, R. Krishna, H. Li, S. Xiang, H. Wu, J. Li, W. Zhou and B. Chen, *Science*, 2018, **362**, 443.
25 Y. Ye, W. Guo, L. Wang, Z. Li, Z. Song, J. Chen, Z. Zhang, S. Xiang and B. Chen, *J. Am. Chem. Soc.*, 2017, **139**, 15604–15607.
26 R.-B. Lin, H. Wu, L. Li, X.-L. Tang, Z. Li, J. Gao, H. Cui, W. Zhou and B. Chen, *J. Am. Chem. Soc.*, 2018, **140**, 12940–12946.
27 Y. Ye, S. Chen, L. Chen, J. Huang, Z. Ma, Z. Li, Z. Yao, J. Zhang, Z. Zhang and S. Xiang, *ACS Appl. Mater. Interfaces*, 2018, **10**, 30912–30918.
28 Y. Fang, S. Banerjee, E. A. Joseph, G. S. Day, M. Bosch, J. Li, Q. Wang, H. Drake, O. K. Ozdemir, J. M. Ornstein, Y. Wang, T.-B. Lu and H.-C. Zhou, *Chem. – Eur. J.*, 2018, **24**, 16977–16982.
29 Y. Ye, L. Zhang, Q. Peng, G. E. Wang, Y. Shen, Z. Li, L. Wang, X. Ma, Q. H. Chen, Z. Zhang and S. Xiang, *J. Am. Chem. Soc.*, 2015, **137**, 913–918.
30 Y. Peng, V. Krungleviciute, I. Eryazici, J. T. Hupp, O. K. Farha and T. Yildirim, *J. Am. Chem. Soc.*, 2013, **135**, 11887–11894.
31 J.-M. Lin, C.-T. He, Y. Liu, P.-Q. Liao, D.-D. Zhou, J.-P. Zhang and X.-M. Chen, *Angew. Chem., Int. Ed.*, 2016, **55**, 4674–4678.
32 Y. He, W. Zhou, T. Yildirim and B. Chen, *Energy Environ. Sci.*, 2013, **6**, 2735–2744.
33 B. Li, H. M. Wen, H. Wang, H. Wu, M. Tyagi, T. Yildirim, W. Zhou and B. Chen, *J. Am. Chem. Soc.*, 2014, **136**, 6207–6210.
34 B. Li, H.-M. Wen, H. Wang, H. Wu, T. Yildirim, W. Zhou and B. Chen, *Energy Environ. Sci.*, 2015, **8**, 2504–2511.
35 H.-M. Wen, B. Li, L. Li, R.-B. Lin, W. Zhou, G. Qian and B. Chen, *Adv. Mater.*, 2018, **30**, 1704792.
36 J. A. Mason, J. Oktawiec, M. K. Taylor, M. R. Hudson, J. Rodriguez, J. E. Bachman, M. I. Gonzalez, A. Cervellino, A. Guagliardi, C. M. Brown, P. L. Llewellyn, N. Masciocchi and J. R. Long, *Nature*, 2015, **527**, 357–361.
37 Q. Y. Yang, P. Lama, S. Sen, M. Lusi, K. J. Chen, W. Y. Gao, M. Shivanna, T. Pham, N. Hosono, S. Kusaka, J. J. T. Perry, S. Ma, B. Space, L. J. Barbour, S. Kitagawa and M. J. Zaworotko, *Angew. Chem., Int. Ed.*, 2018, **57**, 5684–5689.
38 T. Kundu, M. Wahiduzzaman, B. B. Shah, G. Maurin and D. Zhao, *Angew. Chem., Int. Ed.*, 2019, **58**, 8073–8077.
39 T. Kundu, B. B. Shah, L. Bolinois and D. Zhao, *Chem. Mater.*, 2019, **31**, 2842–2847.
40 Y. He, B. Li, M. O'Keeffe and B. Chen, *Chem. Soc. Rev.*, 2014, **43**, 5618–5656.
41 Y. Yan, M. Juricek, F. X. Coudert, N. A. Vermeulen, S. Grunder, A. Dailly, W. Lewis, A. J. Blake, J. F. Stoddart and M. Schröder, *J. Am. Chem. Soc.*, 2016, **138**, 3371–3381.
42 Y. He, S. Xiang, Z. Zhang, S. Xiong, C. Wu, W. Zhou, T. Yildirim, R. Krishna and B. Chen, *J. Mater. Chem. A*, 2013, **1**, 2543–2551.
43 Y. Ye, Z. Ma, L. Chen, H. Lin, Q. Lin, L. Liu, Z. Li, S. Chen, Z. Zhang and S. Xiang, *J. Mater. Chem. A*, 2018, **6**, 20822–20828.
44 T. K. Prasad, D. H. Hong and M. P. Suh, *Chem. – Eur. J.*, 2010, **16**, 14043–14050.
45 M. Zhang, W. Zhou, T. Pham, K. A. Forrest, W. Liu, Y. He, H. Wu, T. Yildirim, B. Chen, B. Space, Y. Pan, M. J. Zaworotko and J. Bai, *Angew. Chem., Int. Ed.*, 2017, **56**, 11426–11430.
46 X. Rao, J. Cai, J. Yu, Y. He, C. Wu, W. Zhou, T. Yildirim, B. Chen and G. Qian, *Chem. Commun.*, 2013, **49**, 6719–6721.
47 X. Duan, J. Yu, J. Cai, Y. He, C. Wu, W. Zhou, T. Yildirim, Z. Zhang, S. Xiang, M. O'Keeffe, B. Chen and G. Qian, *Chem. Commun.*, 2013, **49**, 2043–2045.
48 J. Cai, X. Rao, Y. He, J. Yu, C. Wu, W. Zhou, T. Yildirim, B. Chen and G. Qian, *Chem. Commun.*, 2014, **50**, 1552–1554.
49 M. P. Suh, H. J. Park, T. K. Prasad and D.-W. Lim, *Chem. Rev.*, 2012, **112**, 782–835.
50 J. L. C. Rowsell, A. R. Millward, K. S. Park and O. M. Yaghi, *J. Am. Chem. Soc.*, 2004, **126**, 5666–5667.